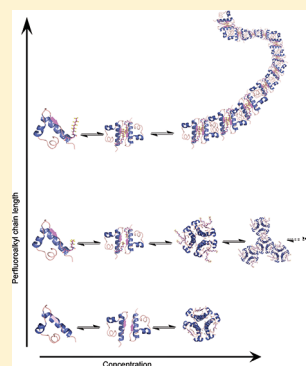


Perfluoroalkyl Chains Direct Novel Self-Assembly of Insulin

Leila Malik,[†] Jesper Nygaard,[†] Rasmus Hoiberg-Nielsen,[†] Lise Arleth,^{†,*} Thomas Hoeg-Jensen,^{‡,*} and Knud J. Jensen^{*,†}[†]IGM, Faculty of Life Sciences, University of Copenhagen, Thorvaldsensvej 40, 1871 Frederiksberg, Denmark[‡]Diabetes Protein and Peptide Chemistry, Novo Nordisk, Park D6.1.142, 2760 Maaloev, Denmark

Supporting Information

ABSTRACT: The self-assembly of biopharmaceutical peptides into multimeric, nanoscale objects, as well as their disassembly to monomers, is central for their mode of action. Here, we describe a bioorthogonal strategy, using a non-native recognition principle, for control of protein self-assembly based on intermolecular fluororous interactions and demonstrate it for the small protein insulin. Perfluorinated alkyl chains of varying length were attached to desB30 human insulin by acylation of the ϵ -amine of the side-chain of LysB29. The insulin analogues were formulated with Zn^{II} and phenol to form hexamers. The self-segregation of fluororous groups directed the insulin hexamers to self-assemble. The structures of the systems were investigated by circular dichroism (CD) spectroscopy and synchrotron small-angle X-ray scattering. Also, the binding affinity to the insulin receptor was measured. Interestingly, varying the length of the perfluoroalkyl chain provided three different scenarios for self-assembly; the short chains hardly affected the native hexameric structure, the medium-length chains induced fractal-like structures with the insulin hexamer as the fundamental building block, while the longest chains lead to the formation of structures with local cylindrical geometry. This hierarchical self-assembly system, which combines Zn^{II} mediated hexamer formation with fluororous interactions, is a promising tool to control the formation of high molecular weight complexes of insulin and potentially other proteins.



INTRODUCTION

The oligomeric state of peptide and protein based pharmaceuticals is essential for their efficacy.¹ One way to address this is to design protein systems that self-organize spontaneously in a well-defined manner by self-assembly under controlled conditions. Insulin is a clear illustration of this, since monomeric insulin is fast-acting, whereas insulin variants that predominantly form insulin hexamers and higher-ordered oligomers are longer-acting. Insulin is most commonly given as subcutaneous injections that form a depot and the biophysical properties of these depots can be exploited to tune insulin delivery.^{2,3} One way to construct higher-order oligomer insulin assemblies using non-covalent insulin hexamers would be to attach ligands that self-assemble in a bioorthogonal manner to form supramolecular species. This could lead to new prolonged-action insulins that provide improved blood glucose control.

Human insulin consists of two peptide segments, the A- and B-chains with 21 and 30 amino acids, respectively, which are connected by two disulfide bridges; a third disulfide bridge is found in the A-chain.⁴ DesB30 insulin (1), which is human insulin without the C-terminal Thr (at position 30 in the B-chain), is the insulin backbone used in insulin detemir.⁵ Insulin exists as a hexamer in the pancreas as well as in drug formulations. The hexameric form consists of a trimer of dimers via coordination of two Zn^{II} atoms. Insulin exists in two hexameric forms known as the T- and R-conformations. The R-conformer is promoted in solution by the presence of phenol, m-cresol or resorcinol.^{6–9} This propensity of

insulin to form hexamers and the ability to use organic chemistry to modify insulin has led to different approaches to obtain long-acting insulin. One approach has been acylation of the ϵ -amino group of residue LysB29 with a long-chain saturated fatty acid to promote binding to circulating serum albumin after injection.^{10,11} Another strategy was the use of N-lithocholyl insulin analogues.¹² These analogues proved to be multihexamers that gave a prolonged effect. The higher-ordered self-assembled structures were dominant in formulations without phenol (insulin T-form).

Here, we present a bioorthogonal approach to create molecular recognition between proteins. The addition of perfluorinated chains to organic molecules changes their physical and chemical properties,¹³ as highly fluorinated molecules tend to segregate into a fluororous phase, a phenomenon which is often referred to as a fluororous effect.¹³ The fluororous effect has been used to direct folding intramolecularly in peptides and proteins, by incorporation of amino acids with fluorinated side-chains.¹⁴ In contrast, placing a perfluoroalkyl group on the surface of a protein could potentially direct intermolecular fluororous self-assembly, which would be a new and bio-orthogonal approach to control the oligomeric state of proteins and enable the formation of soluble macromolecular complexes. Applied to

Received: August 4, 2011

Revised: November 15, 2011

Published: November 30, 2011

insulin, this method could lead to a slow release of insulin analogues into the bloodstream and thereby prolong their effect.

In the present project, we chemically modified insulin with perfluoroalkyl chains of chain-length C₃F₇ to C₉F₁₉. The insulin analogues were then formulated as for ordinary human insulin and other analogues. The secondary structures of the formed aggregates were investigated by means of circular dichroism (CD) spectroscopy while the 3D low resolution structure, hence the topology, were investigated by synchrotron small-angle X-ray scattering.

EXPERIMENTAL METHODS

All organic solvents were obtained from Iris Biotech, Germany. DesB30 human insulin was from Novo Nordisk, Denmark. All fluorinated reagents were obtained from Fluorous Technologies Inc., USA. Analytical HPLC was performed on a Dionex Ultimate 3000 with *Chromleon 6.80SP3* software. Insulin analogues were analyzed on a Phenomenex Gemini 110 Å C18 column (3 μm, 4.6 × 50 mm) and on a Phenomenex Gemini 110 Å C4 column (3 μm, 4.6 × 50 mm), applying a flow of 1.0 mL/min with a linear gradient with increasing amount of buffer B over 10–20 min. Analytical method 1: buffer A: 0.1% formic acid in H₂O; buffer B: 0.1% formic acid in CH₃CN. Analytical method 2: buffer C: 10 mM phosphate in H₂O; buffer D: 10% 100 mM phosphate in CH₃CN, pH 7.4. Preparative HPLC was performed on a Dionex Ultimate 3000 with *Chromleon 6.80SP3* software. Insulin analogues were purified on a FEF 300 Å C4 column (5 μm, 20 × 250 mm), applying a flow of 10.0 mL/min with a linear gradient with increasing amount of buffer (10% B to 100% B) over 37 min (buffer A: 0.1% TFA in H₂O; buffer B: 0.1% TFA in CH₃CN). Mass analysis was performed on an ESI-MS Mass Spectrometer (MSQ Plus, Thermo). ¹H (300 MHz) and ¹³C (75 MHz) NMR spectra were recorded on a Bruker 300 NMR spectrometer with a BBO probe. MS spectra were obtained on a Micro-mass LCT high resolution time-of-flight instrument by direct injection. Ionization was performed in positive electrospray mode. Obtaining mass spectra of perfluorinated compounds is notoriously difficult. However, for the homologous series perfluoroalkyl NHS esters 1–6, satisfying mass spectra were obtained for 3, 4, and 5.

General Procedure for Synthesis of Succinimide Ester. *2,5-Dioxopyrrolidine-1-yl 4,4,5,5,6,6,6-heptafluorohexanoate 1.* 2*H,2H,3H,3H*-Perfluorohexanoic acid (242 mg, 1 mmol) was dissolved in THF (3 mL), then TSTU (361 mg, 1.2 mmol) and DIEA (205 μL, 1.2 mmol) were added. The reaction mixture was stirred overnight at room temperature, evaporated to dryness, dissolved in ethyl acetate (50 mL), and washed with 0.1 M HCl (50 mL) and then water (50 mL). The organic phase was dried over MgSO₄ and evaporated to dryness, yield 140 mg (41%). ¹H NMR (CD₃)₂SO δ 3.0 (2H, t), 2.8 (4H, s), 2.52–2.48 (2H, m). ¹³C NMR (CD₃)₂SO δ 169.7 (C=O amide), 167.7 (C=O ester), 25.4 (CH₂), 25.2 (CH₂–CH₂), 22.2 (CH₂).

2,5-Dioxopyrrolidine-1-yl 4,4,5,5,6,6,7,7,7-nonafluoroheptanoate 2. Compound 2 was prepared by reaction of 2*H,2H,3H,3H*-perfluoroheptanoic acid (292 mg, 1 mmol) with TSTU (361.3 mg, 1.2 mmol) and DIEA (205 μL, 1.2 mmol) overnight in THF (3 mL) according to the general procedure, yield 132 mg (34%). ¹H NMR (CD₃)₂SO δ 3.0 (2H, t), 2.8 (4H, s), 2.51–2.48 (2H, m). ¹³C NMR (CD₃)₂SO δ 168.7 (C=O amide), 166.7 (C=O ester), 26.1 (CH₂), 25.6 (CH₂–CH₂), 22.8 (CH₂).

2,5-Dioxopyrrolidine-1-yl 4,4,5,5,6,6,7,7,8,8,9,9,9-dodecafluoro-8-(trifluoromethyl)nonanoate 3. Compound 3 was prepared by reaction of 2*H,2H,3H,3H*-perfluoro-8-methylnonanoic acid (500 mg, 1.13 mmol) with TSTU (409 mg, 1.36 mmol) and DIEA (232 μL, 1.36 mmol) overnight in THF (3 mL) according to the general procedure, yield 214 mg (35%). ¹H NMR CDCl₃ δ 2.9 (2H, t), 2.8 (4H, s), 2.59–2.41 (2H, m). ¹³C NMR (CD₃)₂SO δ 176.8 (C=O amide), 172.3 (C=O ester),

26.2 (CH₂), 25.3 (CH₂–CH₂), 25.2 (CH₂). MS, calculated average isotopic composition for C₁₄H₃F₁₅NO₄, 539.0 Da; found: *m/z* 561.9 [M+Na].

2,5-Dioxopyrrolidine-1-yl 4,4,5,5,6,6,7,7,8,8,9,9,9-tridecafluorononanoate 4. Compound 4 was prepared by reaction of 2*H,2H,3H,3H*-perfluorononanoic acid (500 mg, 1.28 mmol) with TSTU (461 mg, 1.2 mmol) and DIEA (261 μL, 1.53 mmol) overnight in THF (3 mL) according to the general procedure, yield 238 mg (38%). ¹H NMR CDCl₃ δ 2.9 (2H, t), 2.8 (4H, s), 2.59–2.41 (2H, m). ¹³C NMR (CD₃)₂SO δ 168.7 (C=O amide), 166.7 (C=O ester), 26.2 (CH₂), 25.6 (CH₂–CH₂), 22.8 (CH₂). MS, calculated average isotopic composition for C₁₃H₈F₁₅NO₄, 489.0 Da; found: *m/z* 511.9 [M+Na].

2,5-Dioxopyrrolidine-1-yl 4,4,5,5,6,6,7,7,8,8,9,9,10,10,11,11,11-heptadecafluoroundecanoate 5. Compound 5 was prepared by reaction of 2*H,2H,3H,3H*-perfluoroundecanoic acid (492.1 mg, 1 mmol) with TSTU (361 mg, 1.2 mmol) and DIEA (205 μL, 1.2 mmol) overnight in THF (3 mL) according to the general procedure, yield 241 mg (41%). ¹H NMR CDCl₃ δ 2.90 (2H, t), 2.79 (4H, s), 2.60–2.42 (2H, m). ¹³C NMR CDCl₃ δ 168.7 (C=O amide), 166.7 (C=O ester), 26.2 (CH₂), 25.6 (CH₂–CH₂), 22.8 (CH₂). MS, calculated average isotopic composition for C₁₅H₈F₁₇NO₄, 589.0 Da; found: *m/z* 611.9 [M+Na].

2,5-Dioxopyrrolidine-1-yl 4,4,5,5,6,6,7,7,8,8,9,9,10,11,11,11-hexadecafluoro-10-(trifluoromethyl)undecanoate 6. Compound 6 was prepared by reaction of 2*H,2H,3H,3H*-perfluoro-10-methylundecanoic acid (542 mg, 1 mmol) with TSTU (361 mg, 1.2 mmol) and DIEA (205 μL, 1.2 mmol) overnight in THF (3 mL) according to general procedure. Yield 305 mg (52%). ¹H NMR CDCl₃ δ 2.99 (2H, t), 2.88 (4H, s), 2.68–2.51 (2H, m). ¹³C NMR CDCl₃ δ 168.7 (C=O amide), 166.7 (C=O ester), 26.2 (CH₂), 25.6 (CH₂–CH₂), 22.8 (CH₂).

General Procedure for Synthesis of Perfluoroalkyl Insulin Analogues. *B29N^ε-2H,2H,3H,3H-Perfluorohexanoyl DesB30 Human Insulin DesB30-C₃F₇.* DesB30 human insulin (1, 200 mg, 35 μmol) was dissolved in 0.1 M aq. Na₂CO₃ (2 mL) at pH 10.5, then active ester 2,5-dioxopyrrolidine-1-yl 4,4,5,5,6,6,6-heptafluorohexanoate (1, 16.4 mg, 42 μmol) dissolved in CH₃CN (2 mL) was added. The pH was measured again to ensure a value of >10, for LysB29-selective acylation. After 45 min the reaction mixture was quenched with 0.2 M methylamine and the crude product was precipitated by adjustment of pH to 5.5 using 0.1 M aq. HCl. Centrifugation afforded crude material which was dissolved in water (due to solvability concern the pH was adjusted to 8.2 using 0.1 M Na₂CO₃) and then purified by reverse phase HPLC (C4 column, water/CH₃CN/0.1% TFA). Insulin derivative DesB30-C₃F₇ was isolated by lyophilization, yielding 32.5 mg (16%). Analytical HPLC method 1: purity >98%. Analytical HPLC method 2: purity 97%. ESI-MS, calculated average isotopic composition for C₂₅₉H₃₇₉F₇N₆₄O₇₆S₆, 5930.5 Da; found: *m/z* 1483.5 [M+4H]⁴⁺, 1186.7 [M+5H]⁵⁺.

B29N^ε-2H,2H,3H,3H-Perfluoroheptanoyl DesB30 Human Insulin DesB30-C₄F₉. Synthesis was performed according to the general procedure. Analytical method 1: purity >98%, analytical method 2: purity 98%, yield 38.5 mg (18%). ESI-MS, calculated average isotopic composition for C₂₆₀H₃₇₉F₉N₆₄O₇₆S₆, 5980.5 Da; found: *m/z* 1994.4 [M+3H]³⁺, 1495.5 [M+4H]⁴⁺, 1196.5 [M+5H]⁵⁺.

B29N^ε-2H,2H,3H,3H-Perfluoro-8-methyl-nonanoyl DesB30 Human Insulin DesB30-C₆F₁₃. Synthesis was performed according to the general procedure. Analytical method 1: purity >98%, analytical method 2: purity 96%. Yield 21.5 mg (10%). ESI-MS, calculated average isotopic composition for C₂₆₂H₃₇₉F₁₃N₆₄O₇₆S₆, 6080.6 Da; found: *m/z* 1520.5 [M+4H]⁴⁺, 1216.9 [M+5H]⁵⁺.

B29N^ε-2H,2H,3H,3H-Perfluorononanoyl DesB30 Human Insulin DesB30-C₇F₁₅. Synthesis was performed according to the general procedure. Analytical method 1: purity >98%, analytical method 2: purity 96%, yield 13.8 mg (6%). ESI-MS, calculated average isotopic composition for C₂₆₃H₃₇₉F₁₅N₆₄O₇₆S₆, 6130.6 Da; found: *m/z* 1533.2 [M+4H]⁴⁺, 1226.9 [M+5H]⁵⁺.

B29N^f-2H,2H,3H,3H-Perfluoro-undecanoyl DesB30 Human Insulin DesB30-C₈F₁₇. Synthesis was similar to compound DesB30-C₃F₇. Analytical method 1: purity >98%, analytical method 2: purity 96%. Yield 8.4 mg (4%). ESI-MS, calculated average isotopic composition for C₂₆₄H₃₇₉F₁₇N₆₄O₇₆S₆, 6180.6 Da, found: *m/z* 1546.3 [M+4H]⁴⁺, 1237.2 [M+5H]⁵⁺.

B29N^f-2H,2H,3H,3H-Perfluoro-10-methyl-undecanoyl DesB30 Human Insulin DesB30-C₉F₁₉. Synthesis was performed according to the general procedure. Analytical method 1: purity >97%, analytical method 2: purity 98%. Yield 18.8 mg (8%). ESI-MS, calculated average isotopic composition for C₂₆₅H₃₇₉F₁₉N₆₄O₇₆S₆, 6230.6 Da, found: *m/z* 1520.5 [M+4H]⁴⁺, 1216.9 [M+5H]⁵⁺.

V8 Treatment to Verify the LysB29 Acylation. DesB30-C₃F₇ and DesB30-C₉F₁₉ (1 mg) in phosphate buffer (0.1M, pH 7.5, 300 mL) was treated with V8 glutamyl endopeptidase (6 mL, 1 mg/mL, 2%, w/w). The mixture of peptide fragments was then analyzed by LC-MS, which proved the expected acylation of LysB29.

Insulin Receptor Binding Assay. Binding of the insulin analogues to the insulin receptor (IR) was determined by competition of [125I]TyrA14-labeled insulin binding in a scintillation proximity assay (SPA) as recently published¹⁵ and data from the SPA were analyzed according to the four-parameter logistic model assuming a common slope, basal and maximal response level of the curves for human insulin and the insulin analogues. The percentage of tracer bound in the absence of competing ligand was less than 15% in all assays, to prevent ligand-depletion artifacts, and ~14-fold changes in responses were obtained. The affinities (picomolar affinity range) of the analogues are calculated relative to that of human insulin [IC₅₀(insulin)/IC₅₀(analogue) × 100%] measured within the same plate.

Circular Dichroism (CD) Spectroscopy. Insulin analogues were dissolved in 100 mM Tris buffer, pH 8.0. Concentrations were determined by UV absorbance using a molecular absorption coefficient, ε₂₈₀ of 5730 M⁻¹ cm⁻¹. Far-UV CD data were recorded on a JASCO J815 calibrated with ammonium d-10-camphorsulfonate (ACS). All spectra were recorded at room temperature using a 0.01 cm cell path length and a peptide concentration of about 1 mg/mL. The result Δε is based on the molar concentration of peptide bond.

Small Angle X-ray Scattering (SAXS). Measurements were performed on the I711 small-angle X-ray scattering beamline at MaxLab, Lund, Sweden.¹⁶ All samples of perfluoroalkyl insulin analogues were prepared according to a standard method for insulin sample preparation. Insulin and perfluoroalkyl insulin analogue mixtures were dissolved in CH₃CN:H₂O (1:1) and lyophilized to ensure a homogeneous mixture. Then the samples were dissolved as in standard insulin formulation with a total concentration of 600 μM insulin:perfluoroalkyl insulin, with 2 zinc(II) per hexamer (300 μM), 60 mM phenol, 100 mM NaCl, 7 mM sodium phosphate, pH 7.4. Data were collected on a MARCCD 165 CCD detector. Buffer background measurements were performed before and after each sample measurement and then averaged before being used for background subtraction. All SAXS measurements were performed at 24 ± 1 °C. Water was used for the absolute calibration and checked against DesB30 insulin hexamers (~3 mg/mL).

Using the BioXTAS RAW¹⁷ software, the 2-D CCD images were transformed into the 1-D *I*(*q*) representation where *q* = 4π sin θ/λ, where λ is the X-ray wavelength (λ = 1.1 Å in the present experiment) and θ is the scattering angle.¹⁸ Furthermore, the data were background subtracted and converted into absolute scale units (cm²/cm³) by using water as an external standard. In the process of preliminary data analysis, the obtained scattering intensities, *I*(*q*), were converted into a direct space representation in terms of the pair distance distribution function, *p*(*r*), by means of indirect Fourier transformation using the IFT method based on Bayesian statistics that has been built into BioXTAS RAW. For proteins, which have an almost uniform electron density,¹⁹ the

p(*r*) function can be considered as a histogram of interparticle distances.²⁰ Thus, both the *I*(*q*) and *p*(*r*) plots contain information about the particle shape and size.

Modeling of the Small-Angle Scattering Data. Generally, the scattering, *I*(*q*), from particles in solution can be calculated as a product of form factor, *P*(*q*), describing the scattering from the single particles, an effective structure factor, *S*(*q*), describing the interparticle scattering and a prefactor, *c*, which may be calculated by the product of the concentration of the particles, their molar mass, and their excess scattering length per unit mass.^{18,21}

$$I(q) = c \cdot P(q) \cdot S(q) \quad (1)$$

In order to model the form factor, direct space representations of the different oligomeric forms of insulin were obtained from the Protein Data Bank 3I3Z.pdb for the insulin monomer,²² while the insulin dimer and hexamer were created by use of PyMOL²³ from the 1EV3.pdb structure. Using the *Crysol*²⁴ software the scattering intensities from, respectively, the insulin monomer, dimer, and hexamer were calculated. These numerical representations of the scattering intensities were then used by our Fortran based least-squares fitting routine in combination with a structure factor describing the particle–particle interaction effects. The numerical form factor for the single proteins and the analytical structure factor were combined using Kotlarchyk and Chen's so-called decoupling approximation²⁵ using the same approach as described in a previous article by Høiberg-Nielsen et al.²⁶

Fractal-Like Aggregates Composed of Insulin Subunits.

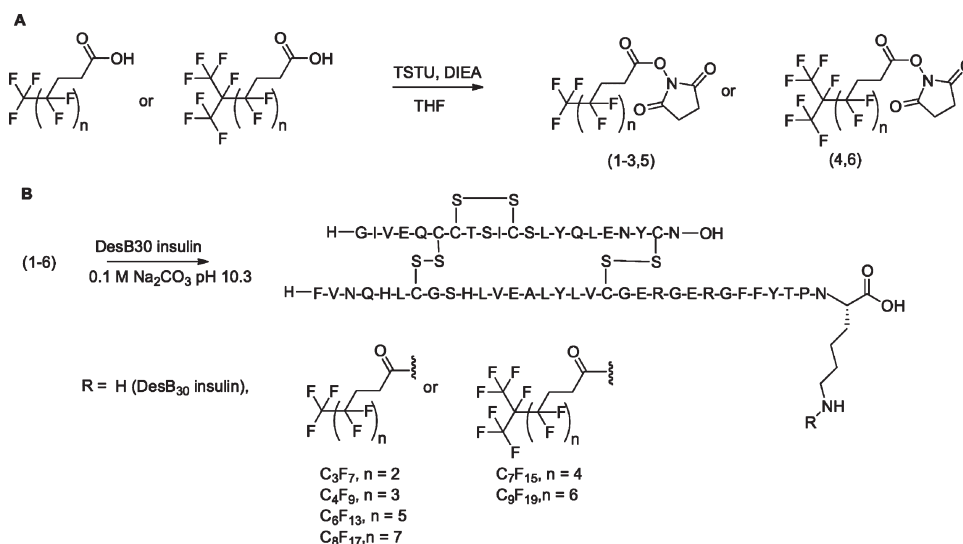
One of our structural hypotheses for the aggregates formed by the perfluoroalkyl insulin conjugates was that the perfluoroalkyl chains would still allow the formation of hexameric insulin complexes, but the attractions between the perfluoroalkyl chains would induce formation of oligomers of hexamers and thus of agglomerates of the insulin. A good structural representation of the small-angle scattering of such agglomerates is the fractal-like structure factor originally developed by Teixeira et al.²⁷ Teixeira's structure factor for fractal aggregates was then combined with a form factor of the single subunits of the agglomerate, in this case the form factor for the insulin. This way the small-angle scattering of, for example, insulin hexamers aggregating into a larger fractal-like aggregate can be mathematically described and subsequently compared to the experimental data. The structure factor for the fractal model is given by eq 2; where *D* is the fractal dimension, *r*₀ is the interaction radius of the subunits in the model, Γ(*x*) is the gamma function, ξ is a correlation length corresponding to the size of the aggregates.

$$S(q) = 1 + \frac{1}{(qr_0)^D} \frac{D\Gamma(D-1)}{\left[1 + 1/(q^2\xi^2)\right]^{(D-1)/2}} \times \sin[(D-1)\tan^{-1}(q\xi)] \quad (2)$$

In the case of weak attraction between the modified insulin analogues, the aggregates will assemble and disassemble in a dynamical fashion and both hexamer aggregates and "monomeric" hexamers will be present in the sample. This situation is taken into account in the modeling by allowing for a microstructure where a fraction, *X*_{SA}, of the insulin is in the form of self-assembled fractal-like aggregates of hexamers and the remaining fraction, (*X*_{hex} = 1 - *X*_{SA}), is in the form of free hexamers.

Particles with Cylindrical Geometry – Short Cylinders. The first fractal model evaluated could not adequately describe the scattering from the insulin with the C₇F₁₅ and C₈F₁₇ chains. Instead the DesB30-C₇F₁₅ and DesB30-C₈F₁₇ insulins were best fitted with a model for particles with local cylindrical geometry. For the DesB30-C₇F₁₅ we used the form factor short cylindrical particles.^{28,29}

$$P_{\text{cylinder}}(q) = \int \left[\frac{2J_1(qR \sin \alpha)}{qR \sin \alpha} \frac{\sin(qL \cos \alpha/2)}{qL \cos \alpha/2} \right]^2 \sin \alpha \, d\alpha \quad (3)$$

Scheme 1^a

^a (A) Synthesis of succinimide esters (1–6). (B) Synthesis of insulin analogues with linear and branched perfluoroalkyl chains at the LysB29 side-chain.

Where $J_1(x)$ is the first-order Bessel function, R is the cross-section radius, and L is the length of the cylinder.

Particles with Cylindrical Geometry – Wormlike Chains.

For DesB30- C_8F_{17} the best model fits, somewhat surprisingly, were obtained with a model for wormlike chains with local cylindrical geometry. The scattering from the semiflexible self-avoiding wormlike chains may be factorized into a term describing the chain cross-section contribution to the scattering, $P_{CS}(q)$, and a term $P_{WC}(q)$, describing the longitudinal contribution to the scattering in terms of a semiflexible wormlike chain.^{30,31}

$$P(q) = P_{CS} \times P_{WC}(q) \quad (4)$$

The contribution to the scattering from the local cylindrical geometry is

$$P_{CS}(q) = \left[\frac{2 \cdot J_1(qR)}{qR} \right]^2 \quad (5)$$

Where $J_1(x)$ is the first-order Bessel function and R is cross-section radius.

The longitudinal contribution to the scattering, $P_{WC}(q)$, was calculated using a previously applied³⁰ numerical expression for the scattering from semiflexible wormlike chains as developed by Pedersen and Schurtenberger.³¹ The expression is based on a series of Monte Carlo simulations of semiflexible polymers with excluded volume effects, performed by Pedersen, Laso, and Schurtenberger.³² The authors simulated a wide range of polymer configurations, sampled them, and calculated and parametrized the corresponding scattering functions, thus obtaining expressions for the scattering functions of semiflexible wormlike micelles in terms of the chain contour length L and the local rigidity as represented by the Kuhn length b .

The structure factor for the particles with cylindrical geometry was assumed to be unity, thus reducing eq 1 to $I(q) = c \cdot P(q)$.

RESULTS

Chemical Synthesis. The succinimidyl esters of six different perfluoroalkyl chains were synthesized and conjugated to the ϵ -amino group of LysB29 DesB30 insulin (Scheme 1A).³³ The pK_a values of the two N-terminal α -amino groups of insulin are

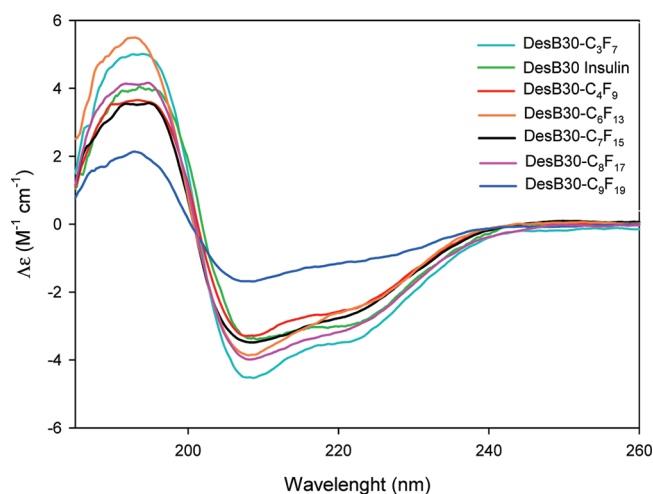


Figure 1. Far-UV CD of the six analogues.

8.4 and 7.1 for GlyA1 and PheB1, respectively, and 11.2 for the ϵ -amino group of LysB29. As a result, the NHS-esters 1–6 can selectively react at LysB29 at high pH (~ 10) to form an amide linkage (Scheme 1B).³⁴ The perfluoroalkyl B29-derivatives were the main products and were purified to homogeneity and analyzed under two different HPLC conditions (see Supporting Information Table S1 for purity and HPLC conditions).

To verify that only LysB29 had been acylated, a V8 glutamyl endopeptidase cleavage was performed on compounds DesB30- C_3F_7 and DesB30- C_9F_{19} followed by HPLC-MS analysis of the fragments, which clearly showed that only the expected LysB29 conjugates were obtained.³⁵

CD Spectroscopy. CD spectroscopy was used to study the secondary structure for any conformational changes after conjugation. The far-UV CD band at 208 nm primarily arises from an α -helical structure, as does the band at 222 nm.³⁶ The spectral characteristics of the perfluorinated insulin analogues with shorter chain length (DesB30- C_3F_7 and DesB30- C_4F_9) were found to be very similar to desB30 insulin. However, CD spectra of insulin

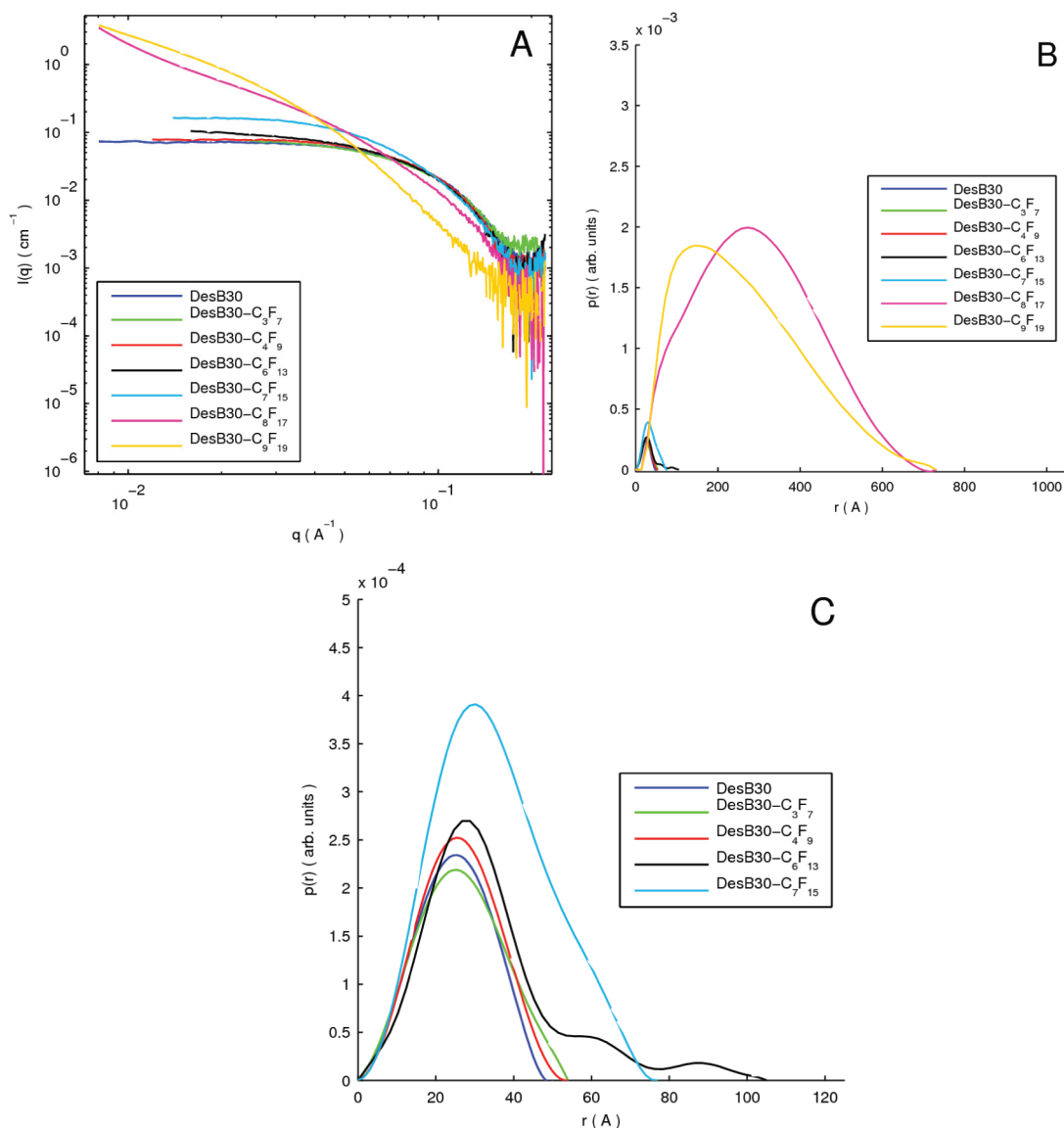


Figure 2. (A) SAXS data of the different perfluoroalkyl-insulin analogues. (B) the corresponding pair distance distribution ($p(r)$ -functions). (C) The $p(r)$ -functions plotted in the region 0–120 Å.

conjugate DesB30-C₉F₁₉ which carries the longest perfluoroalkyl chain, revealed that the substitution had disrupted part of the helical structure of the molecule (Figure 1).

Receptor Binding. The insulin receptor affinities of the six perfluoroalkyl insulin analogues were tested as previously described,³⁷ and the affinities for analogues DesB30-C₃F₇ and DesB30-C₄F₉ were comparable to insulin (93% and 77%, respectively), whereas analogues DesB30-C₆F₁₃ and DesB30-C₇F₁₅ gave 2-fold reductions in binding affinity, 54% and 46%, respectively (see Supporting Information Table S2 for insulin receptor binding affinity). DesB30-C₈F₁₇ and DesB30-C₉F₁₉ had a binding affinity of 9.1% and 6.2%, respectively, compared to human insulin. Thus, when the size of the perfluoroalkyl substituent was increased, the binding affinity decreases in this case. However, a ~10% relative binding still corresponds to an affinity (IC_{50}) in the picomolar range for the insulin receptor and full in vivo potency of insulin analogues has been observed despite lowered in vitro insulin receptor affinities.³⁸

SAXS Measurements. SAXS was used to examine the self-assembly of the insulin analogues which were formulated as above with Zn^{II} and phenol. Hexamer DesB30 insulin was used as a standard. The experimental scattering profiles for DesB30-C₃F₇ and DesB30-C₄F₉ look remarkably similar to insulin DesB30 itself (Figure 2A). This strongly suggests that the hexameric structure of the DesB30 is conserved in these two samples and that the attachment of short perfluoroalkyl chains does not significantly affect the local structure. For the DesB30-C₆F₁₃ the high- q part of the $I(q)$ resembles that of the DesB30, while the low- q part has an increased scattering intensity. This indicates the formation of larger aggregates build from hexameric subunits. For DesB30-C₇F₁₅, DesB30-C₈F₁₇, and DesB30-C₉F₁₉, the scattering intensity of the low- q region increases even further and a clear trend of an increasing fraction of self-assembled hexamers with increasing fluorine-content can be seen for the perfluoroalkyl insulins. $I(q)$ data for DesB30-C₇F₁₅, DesB30-C₈F₁₇, and DesB30-C₉F₁₉ furthermore shows that the

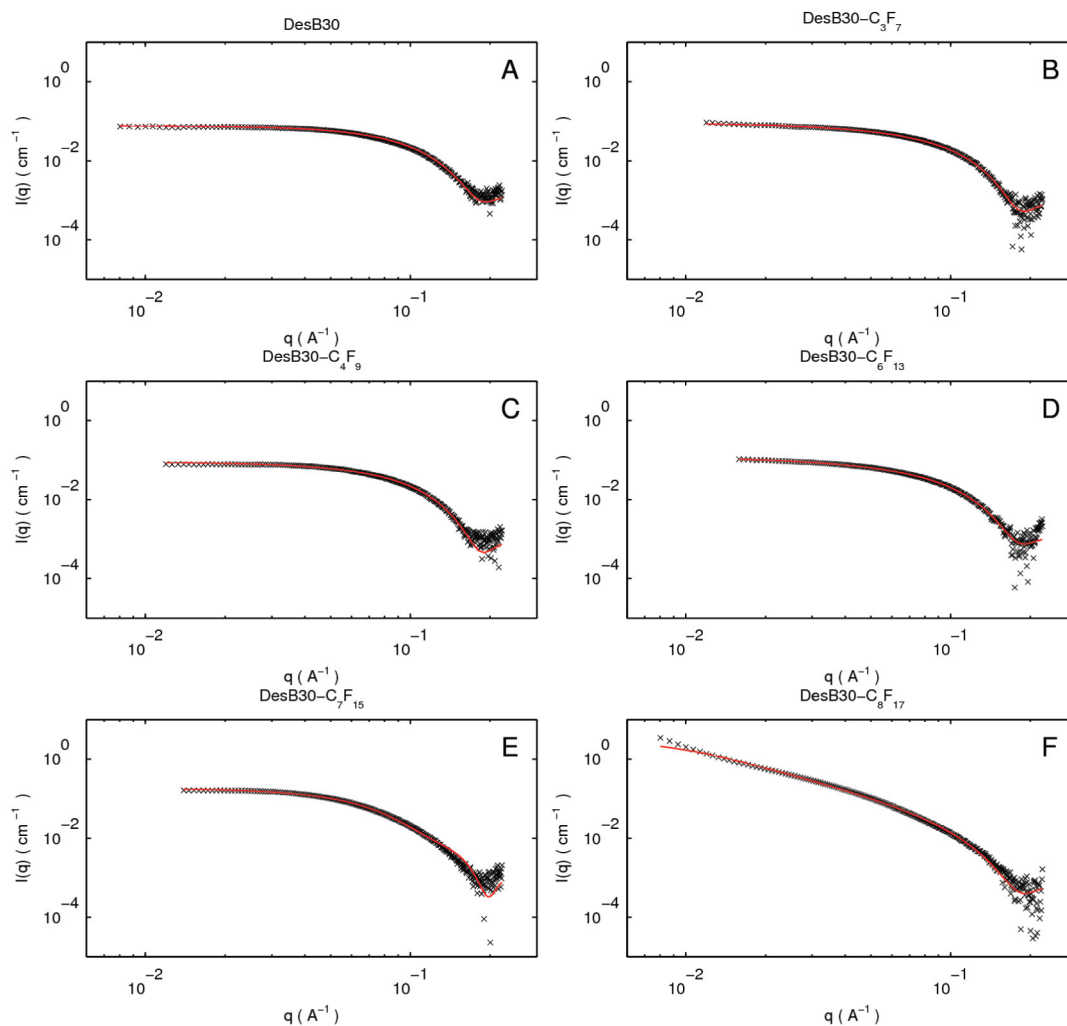


Figure 3. SAXS data and model fits. (A) Des-B30 insulin fitted with the model for insulin hexamers. (B) DesB30-C₃F₇, (C) DesB30-C₄F₉, and (D) DesB30-C₆F₁₃ are all fitted with the model for an insulin hexamer as the basic unit combined with a structure factor for fractal aggregates of insulin hexamers. (E) DesB30-C₇F₁₅ fitted with model for short cylinders. (F) DesB30-C₈F₁₇ fitted with a model for Gaussian chains with local cylindrical geometry.

high- q region gradually deviates more and more from that of the pure DesB30 insulin. This indicates that the larger aggregates are no longer composed of the hexameric subunits.

This set of observations is also reflected in the pair distance distribution functions ($p(r)$ -functions) obtained from the indirect Fourier transformed data (IFT) (Figure 2B).²⁰ Here the nearly bell shaped $p(r)$ -functions for DesB30 insulin and analogues DesB30-C₃F₇ and DesB30-C₄F₉ look very similar, with a D_{max} of approximately 50 Å, and indicate a compact and close to spherical structure as is seen for hexameric insulin. The $p(r)$ -function for analogue DesB30-C₆F₁₃ is still bell-shaped at low r values but with a significant tail at high r values indicating the formation of larger assemblies with the hexamer as the subunit, as illustrated in Figure 5. The $p(r)$ -function for analogue DesB30-C₇F₁₅ clearly differs from that of the desB30 insulin, revealing the formation of even larger molecular self-assemblies.

Taken together, the visual inspection of scattering profiles and the $p(r)$ -functions for the six perfluoro-insulin analogues demonstrated that the sizes of the assemblies increase with the number of fluorine atoms in the perfluoroalkyl chains, which can be seen from increasing $I(0)$ or larger $p(r)$ curve area.

Structural Modeling of the Aggregates. The above-described visual inspection of the experimental scattering functions and the derived pair-distance distribution functions indicate that the aggregates formed by the analogues with short perfluoroalkyl chains have hexamers as their building blocks, while another and probably less ordered microstructure is predominant in the aggregates with long perfluoroalkyl chains. A series of structurally based simulations and corresponding model fits were performed to test these conclusions in a more quantitative way. For the structural modeling we assumed that the insulin was in the form of monomers, dimers, or hexamers and that these would then constitute the basic building blocks of larger aggregates. We furthermore assumed that the formed larger aggregates were randomly structured agglomerates of the subunits. As described above, such structures have previously been successfully described by the so-called Fractal structure factor model developed by Teixeira et al.²⁷ In addition to these intuitively expected structures we tried to fit some of the data with form factors corresponding to polydisperse spheres, discs, and rigid and flexible rods.

Rewardingly, it was possible to fit the three data sets with attached short perfluoroalkyl chains (DesB30-C₃F₇, DesB30-C₄F₉,

Table 1. Model Results for the Short Perfluoroalkyl Insulins^a

ID	$X_{SA}/\%$	$X_{Hex}/\%$	ξ [Å]	D_{frac}
DesB30	0	100	n.a.	n.a.
DesB30-C ₃ F ₇	30 ± 4	70	42 ± 11	1.13 ± 0.33
DesB30-C ₄ F ₉	9 ± 1	91	42 ^b	1.13 ^b
DesB30-C ₆ F ₁₃	59 ± 5	41	42 ^b	1.06 ± 0.04

^a Hexamer subunits organized in fractal-like aggregates. X_{SA} : Fraction of hexamers self-assembled into a fractal-like structure. X_{Hex} : Fraction of non-self-assembled hexamers calculated as $(1 - X_{SA})$. ξ : The correlation length of the aggregates. D_{frac} : The fractal dimension. ^b Parameter set manually.

and DesB30-C₆F₁₃) with a model where we assumed that a fraction of the hexamers were organized in a fractal-like structure, while the remaining part was still in the form of free hexamers (Figure 3A,B,C,D). However, for the particles with the longest perfluoroalkyl chains (DesB30-C₇F₁₅, DesB30-C₈F₁₇, and DesB30-C₉F₁₉) all our attempts to describe the data as resulting from aggregates composed from insulin subunits broke down, when we assumed insulin monomers, dimers, and hexamers as the basic building blocks. The most likely explanation is that the oligomeric form of the insulin is no longer well-defined due to the very strong attraction between the perfluoroalkyl chains. Instead we sought to get a picture of the overall geometry of the formed aggregates by fitting the form factors corresponding to the above-mentioned different-shaped particles to the data. Interestingly, for DesB30-C₇F₁₅ and DesB30-C₈F₁₇ we found a good agreement between the experimental data and, respectively, a model for short cylinders and a model for Gaussian chains with local cylindrical geometry (Figure 3E,F). We were not able to obtain satisfactory fits to the scattering data from the DesB30-C₉F₁₉ sample, i.e., the sample with the longest attached perfluoroalkyl chain, with any of the models.

Samples with Insulin Self-Assembled into a Fractal Like Structure. DesB30-C₆F₁₃ was fitted with the fractal-like model (Table 1), with the fraction of self-assembled hexamers (X_{SA}) fixed to 1. This gave a correlation length, ξ , around 42 Å and a fractal dimension, D_{frac} , of 1.06. Thus a fractal structure with a correlation length of the approximate size of the insulin hexamer and a slightly branched structure. DesB30-C₃F₇ and DesB30-C₄F₉, both exhibited a lower fraction of self-assembly than DesB30-C₆F₁₃. In order to avoid overparametrizing the data, D_{frac} was fixed to the value obtained for DesB30-C₆F₁₃ such that only the fraction of hexamers self-assembled into a fractal-like structure, X_{SA} , and the correlation length, ξ , were fitted. For the DesB30-C₄F₉, ξ , also had to be fixed in order to limit the degree of freedom in the model fits and was set to the value found for DesB30-C₆F₁₃.

For DesB30-C₃F₇, ξ was found to be 42 Å, which is comparable to, however, slightly smaller than the size of the insulin hexamer. X_{SA} was found to be 30% giving a smaller fraction of self-assembled hexamers compared to DesB30-C₆F₁₃. With a X_{SA} of 9% DesB30-C₄F₉ is, somewhat surprisingly, the perfluoroalkyl insulin investigated with the lowest fraction of self-assembled hexamers.

Samples with Insulin Aggregated into a Local Cylindrical Structure. The SAXS data from the DesB30-C₇F₁₅ and DesB30-C₈F₁₇ insulins could not be fitted with the model for fractal-like aggregates: neither when the hexameric subunits were applied, as for the short perfluoroalkyl insulins, nor when the insulin monomer or dimers were used as the subunits. Instead different simple geometrical models (spheres, ellipsoidal discs, cylinders,

Table 2. Model Results for the Long Perfluoroalkyl Chain Insulins^a

ID	R_{chain} [Å]	L [Å]	b_{Kuhn} [Å]
DesB30-C ₇ F ₁₅	20.9 ± 0.1 ^b	66.1 ± 0.2 ^b	n.a.
DesB30-C ₈ F ₁₇	20.2 ± 0.6 ^c	3600 ± 1000 ^c	22.5 ± 8.4 ^c

^a Self-assembly into cylindrical and worm-like structures. ^b Short cylindrical rods. ^c Worm-like chains with cylindrical cross-section. R_{chain} : Cross-sectional radius of the cylinder. L : contour length of the cylinder. b_{Kuhn} : The Kuhn length of the worm-like chains. ^d Parameter set manually.

wormlike chains) were tried. The best agreement between model and experimental data was obtained when using a model for insulin aggregates having, respectively, cylindrical and wormlike structures. In the case of DesB30-C₇F₁₅ a cylinder radius slightly larger than a dimer but smaller than a hexamer was found. As can be seen from Figure 3E DesB30-C₇F₁₅ has a Guinier region, which fits well with that the model fit gives a well-determined average cylinder length, L , of no more than 66 Å (Table 2). The DesB30-C₈F₁₇ particles have approximately the same radius as the DesB30-C₇F₁₅ particles, but are much longer. The attractions introduced by the C₈F₁₇-appendix lead to the assembly of very elongated wormlike chains. A good model-fit could be obtained with a chain-length of about 3600 and a Kuhn length of 22.5 Å (Table 2). Mathematically, there was a strong internal correlation between the chain length and the Kuhn length in the model-fits; this gave rise to relatively large error bars on the obtained values for these two parameters. However, the average radius of the chain could be determined with great accuracy.

Interpretation of the SAXS data suggested a structural behavior of the different insulin analogues as a function of the perfluoroalkyl chain length as is illustrated in Figure 5. Insulins with short perfluoroalkyl chains have a hexameric structure similar to human insulin. As the length of the perfluoroalkyl chains increases, attraction between the hexamers is introduced leading to a fractal-like structure with the hexamer as the fundamental building block. With a further increase in the length of the perfluoroalkyl chain, the fluororous interactions increase further and surpass the interactions that lead to hexamer formation. This leads to a breakdown of the hexameric substructure and the appearance of a wormlike structure. How can the formation of such a chainlike structure with subunits smaller than the hexamer be explained? A simple explanation would be that the chain is held together by alternation between the insulin dimer interactions and the fluororous interactions. This hypothetical structure is illustrated in Figure 5.

Self-Assembly by Formation of Mixed Aggregates of Perfluoroalkyl Modified and Nonmodified Insulin. Based on these observations we studied whether an additional level of control of self-assembly could be introduced by forming hexamers consisting of a mixture of fluoroalkyl insulins and unmodified insulin such that hexamers would have fewer fluororous contact points. This approach would potentially give a distribution of different hexamers.

Using this approach, the possibility of controlling the formation of large assemblies formed by DesB30-C₉F₁₉ insulin was investigated. A series of formulations of a mixture of unmodified insulin and analogue DesB30-C₉F₁₉ were prepared with Zn^{II} and phenol, such that the ratio was always optimal for hexamer formation regarding Zn^{II} and phenol. The SAXS data and the corresponding $p(r)$ -functions obtained are shown in Figure 4A and B.

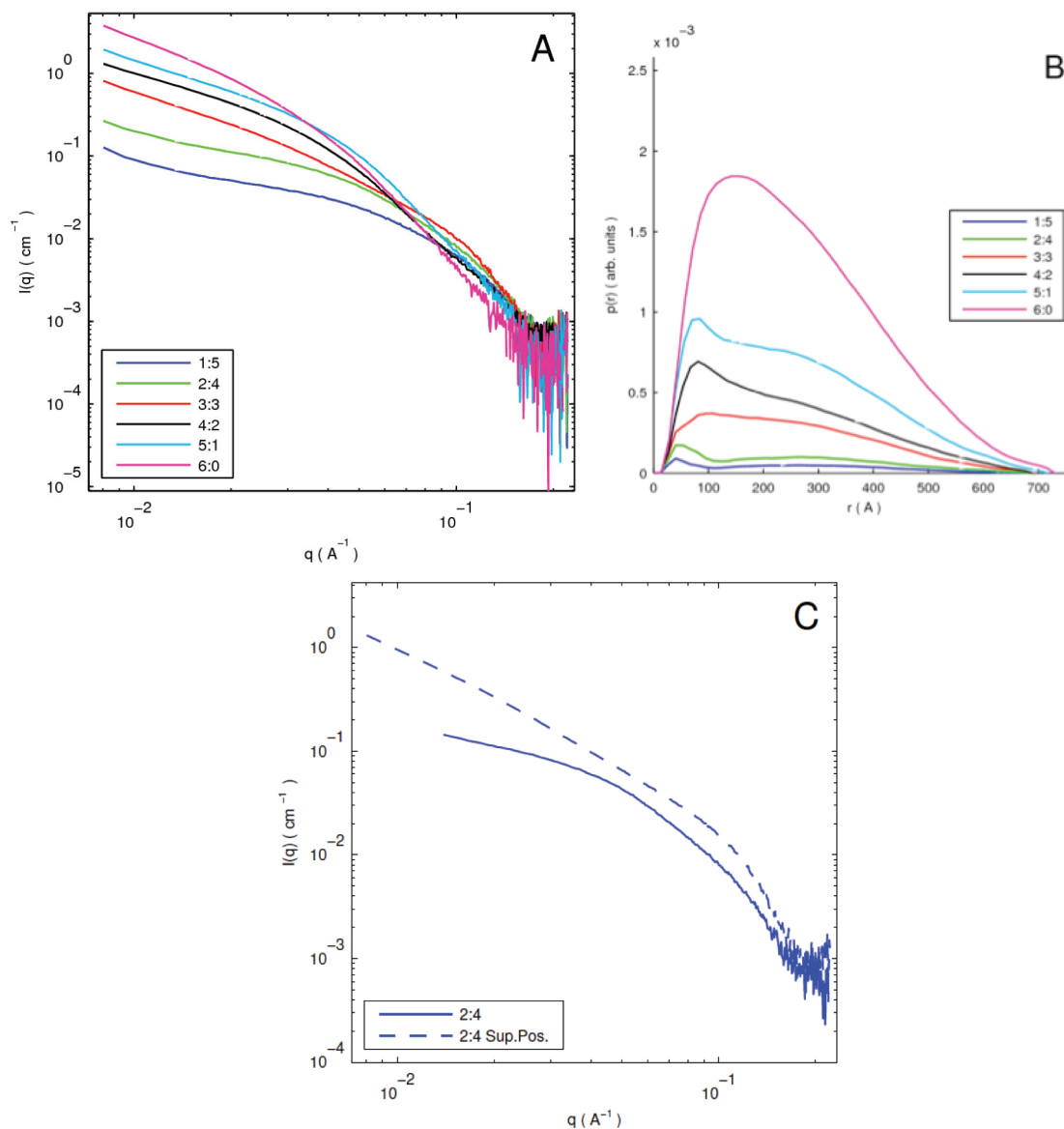


Figure 4. (A) SAXS data from the mixtures of unmodified DesB30 insulin and perfluoroalkyl insulin DesB30-C₉F₁₉ with IFT fit. (B) The corresponding $p(r)$ -functions. (C) SAXS data for the DesB30-C₉F₁₉:DesB30 insulin (2:4) mixture, solid line: experimental data, broken line the superposition of the SAXS data obtained from pure DesB30 and DesB30-C₉F₁₉ combined. The fact that the experimental data for the mixture differs from the combined data for DesB30 and DesB30-C₉F₁₉ indicates that the DesB30 and DesB30-C₉F₁₉ mixture does not self-segregate but forms a mixture at the molecular level.

In both the $I(q)$ functions and in the derived $p(r)$ -functions it was clearly seen that the average size of the aggregates increased with higher proportion of fluoro-insulin analogue DesB30-C₉F₁₉ in the mixture (Figure 4). The absence of a well-defined Guinier range in the $I(q)$ data, however, made it difficult to accurately quantify the maximal size of the formed aggregates. Nevertheless, our data clearly demonstrated that the formation of large assemblies formed by analogue DesB30-C₉F₁₉ can to some extent be controlled by dilution with unmodified desB30 insulin to provide hexamers with <1 fluororous contact point per hexagonal face. However, in the case of the very strong attractions induced by the C₉F₁₉ chains, this dilution was not sufficient to reintroduce an ordered hierarchical structure based on, for example, the hexameric insulin structure as the main building block.

It might be speculated that the strong attraction introduced by the perfluoroalkyl chains in insulin DesB30-C₉F₁₉ could lead to a total segregation between the unmodified and perfluoroalkyl insulin.

In this case the SAXS data of a mixed sample should simply be a superposition of the SAXS data from the unmodified and perfluoroalkyl insulin analogues weighted by their relative concentrations. That this is certainly not the case is clearly shown from Figure 3C. The data for the DesB30-C₉F₁₉:DesB30 insulin (2:4) mixture (Figure 4C blue line) was compared to an appropriately weighted superposition of the SAXS data obtained from the two pure mixtures, thus pure DesB30 (2/6 part) and pure DesB30-C₉F₁₉ (4/6 part) (Figure 4 blue dashed line). As is clearly seen in Figure 4C neither the low- q nor the high- q part of the data curves agree with the superpositioned data. We take this as a clear indication that the two types of insulin do actually form mixed aggregates.

DISCUSSION

Insulin readily forms dimers as well as well-defined hexamers by complexation with two Zn^{II} ions, which can occur in two

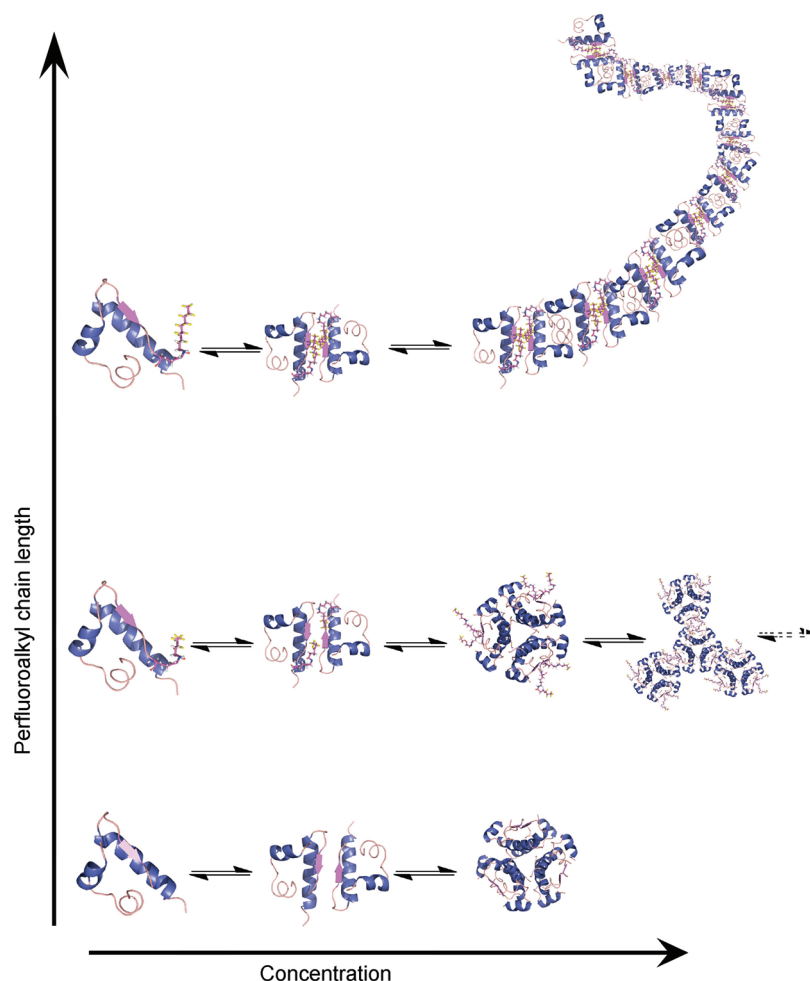


Figure 5. Illustration of perfluoroalkyl insulin self-assembly. Bottom: DesB30 insulin. Middle: DesB30 insulin with medium length perfluoroalkyl chains. Top: Insulin with long perfluoroalkyl chains assembling into cylindrical structures of insulin dimers.

states. The oligomeric state of new insulin variants, i.e., whether they are preferably monomer/dimer or hexamer or multimers of hexamers, determines whether they are fast-acting or slow-acting in the treatment of diabetes. Several insulin variants in clinical use contain a prosthetic group at Lys B29, for example, lipid moieties for binding to human serum albumin and to promote formation of higher aggregates. Insulin is thus a highly interesting model protein for the evaluation of new principles to control intermolecular self-assembly. The C-terminal Thr of the B-chain in insulin (ThrB30) is not essential for binding, and human insulin desB30 has been used in the clinic. The tendency of highly fluorinated molecules to avoid contact with hydrophilic and hydrophobic surfaces and to prefer contact with fluorinated groups leads to a self-segregation which is often referred to as the fluorous effect. This has been used for the isolation and handling of small molecules, as well as to direct the intramolecular folding of peptides and proteins.¹⁴ In contrast, in this project we incorporated perfluoroalkyl moieties on the surface of a small protein, insulin, to direct and control the *intermolecular* self-assembly, hence the quaternary structure. Here, a series of insulin variants functionalized with perfluoroalkyl chains, C₃F₇ to C₉F₁₉, were synthesized by pH controlled regioselective acylation of the Lys side-chain of B29 of desB30 human insulin. These six new insulin variants were then analyzed for their insulin

receptor binding, their secondary structure, and their self-assembly into larger structures.

Insulin variants carrying the perfluoroalkyl chains C₃F₇, C₄F₉, C₆F₁₃, and C₇F₁₅ had insulin receptor affinities of 93–46% compared to human insulin. This is still in the picomolar range and the somewhat lowered affinities are not detrimental. The analogues carrying C₈F₁₇ and C₉F₁₉ chains had affinities of 9.1% and 6.2%, respectively, compared to human insulin. Thus, perfluoroalkyl modification can be compatible with maintaining receptor binding. These values are also comparable to a recently published paper on metal ion mediated self-assembly of insulin derivatives carrying a bipyridine ligand.³⁹

A comparison of the CD spectra of the six perfluoroalkyl DesB30 insulin variants indicated that only the insulin carrying the longest perfluoroalkyl chain, C₉F₁₉, had a significantly lowered degree of α -helicity. The other variants had helicities similar to human insulin or only slightly lower, which was encouraging.

Analysis of the SAXS data of the insulin variants carrying short perfluoroalkyl chains (C₃F₇, C₄F₉, and C₆F₁₃) revealed that the sizes of the assemblies increased with the number of fluorine atoms in the perfluoroalkyl chains. A more detailed structural modeling based data analysis further suggested that the hexameric subunits were conserved as basic building blocks up to a

perfluoroalkyl chain length of C₆F₁₃. However, with longer perfluoroalkyl chain length, a breakdown of the hexameric substructure was observed and instead a new structure, apparently with local cylindrical geometry, became dominating, as illustrated in Figure 5. This new cylindrical geometry was observed for DesB30-C₇F₁₅ and DesB30-C₈F₁₇ and we observed that the increased molecular attraction introduced by the longer perfluoroalkyl chains also gave rise to a significant increase in the overall length of the cylindrical structures. Thus, it seems that with short perfluoroalkyl appendices the hexameric subunit core is still conserved as the dominant structure, whereas with longer perfluoroalkyl appendices, it breaks down and the fluororous interactions start to override and promote intermolecular self-assembly leading to larger structures in combination with a breakdown of the local hexameric structure.

We were not able to make any satisfactory fits to the scattering data from the DesB30-C₉F₁₉ sample with any of the models. A possible explanation could be that the sample is composed of different types of insulin subunits and that the overall structure, as a result of the very strong interaction introduced by the C₉F₁₉, becomes disordered. This again indicates that the very strong fluororous interaction overrules the formation of hexamer constructs leading to the formation of larger aggregates. Thus, the C₉F₁₉ chain may not be useful for controlling protein self-assembly, if it is used as a uniform modification. However, a different approach for using the C₉F₁₉ modification was designed, where unmodified human insulin desB30 was mixed with human insulin DesB30-C₉F₁₉ in different ratios to study whether structural control could be regained by molecular dilution of the DesB30-C₉F₁₉ with unmodified desB30. Indeed, SAXS data indicated that the unmodified insulin and insulin formed mixed oligomers; however, this molecular dilution was, according to our interpretation, not sufficient to reintroduce more well-ordered structures.

The perfluoroalkyl moiety serves a different purpose than a lipid chain on a protein, as the latter promotes binding to hydrophobic surfaces such as serum albumin, while the former uses the fluororous interactions to promote intermolecular self-assembly. These results indicate that modification of proteins with a perfluoroalkyl moiety can indeed be used to intermolecularly assemble them. Importantly, the size of the perfluoroalkyl group provides a level of control. Longer perfluoroalkyl chains could in the present study override metal ion mediated self-assembly and gave cylindrical structures composed of insulin dimers, whereas medium-length perfluoroalkyl chains gave fractal-like assemblies composed of insulin hexamers. This is illustrated in Figure 5 where we go from DesB30 insulin assembly into hexamers (Figure 5 bottom), and then by tuning the length of the perfluoroalkyl chain, we can create fractal-like structures of hexamers (Figure 5 middle). With further elongation of the perfluoroalkyl chain length we can control the self-assembly into cylindrical structures of insulin dimers (Figure 5 top). This bio-orthogonal approach thus provides a tunable tool for construction of protein superstructures.

Using perfluoroalkyl appendices with different lengths, we were able to establish several different scenarios for control of self-assembly of human insulin, as illustrated in Figure 5. The fluororous self-assembly was combined with native Zn^{II} mediated self-assembly, and amounts to a hierarchical process. As this fluororous strategy is bioorthogonal, it seems likely that it can be transferred to other proteins, for example, in the development of biopharmaceutical drug candidates or for protein material science.

CONCLUSIONS

We have prepared six new insulin variants carrying perfluoroalkyl moieties by regioselective chemical acylation of LysB29 in desB30 insulin at high pH. The perfluoroalkyl chain lengths were varied systematically so that the level of fluororous interactions between the perfluoroalkyl insulins was controlled. The six new insulin variants maintained satisfactory levels of binding to the insulin receptor. All but one of them maintained a high degree of α -helicity, as in human insulin. The self-assembly of the perfluoroalkyl insulin variants was studied by SAXS. We introduced a new and bio-orthogonal concept in intermolecular protein self-assembly, which relies on the self-segregating behavior of perfluoroalkyl moieties. Hierarchical intermolecular self-assembly was achieved by combining classical insulin hexamer formation by addition of Zn^{II} and phenol, with incorporation of perfluoroalkyl-insulins with different perfluoroalkyl chain lengths. Rewardingly, three different types of self-assembly were achieved depending on the size of the perfluoroalkyl group. Relatively short perfluoroalkyl chains did not influence the overall quaternary structure of insulin, whereas the longer perfluoroalkyl chains provided increased degrees of self-association of insulin hexamers. The formation of mixed hexamers of insulins and insulins carrying longer perfluoroalkyl chains provided a further level of control. We envision that this approach can be adapted to other proteins and lead to a new way to control self-assembly of proteins.

ASSOCIATED CONTENT

S Supporting Information. Additional information as described in the text. This material is available free of charge via the Internet at <http://pubs.acs.org>.

AUTHOR INFORMATION

Corresponding Author

*E-mail: kjj@life.ku.dk (K.J.J.); lia@life.ku.dk (L.A.); tshj@novonordisk.com (T.H.-J).

ACKNOWLEDGMENT

A NABIIT grant from DSF is gratefully acknowledged. Dr. Thomas B. Kjeldsen is thanked for insulin receptor affinity assays. Beamtime at the I711 beamline at the MAX-lab synchrotron along with user support from Dr. T. Plivelic are gratefully acknowledged. Jesper C. Westergaard is acknowledged for help with Figure 5.

REFERENCES

- (1) Jorgensen, L.; Hostrup, S.; Moeller, E. V.; Grohgan, H. *Expert Opin. Drug Delivery* **2009**, *6*, 12119–11230.
- (2) Owens, D. R. *Nat. Rev. Drug Discovery* **2002**, *1*, 529–540.
- (3) Cefalu, W. T. *Diabetes Care* **2004**, *27*, 239–246.
- (4) Baker, E. N.; Blundell, T. L.; Cutfield, J. F.; Cutfield, S. M.; Dodson, E. J.; Dodson, G. G.; Hodgkin, D. M. C.; Hubbard, R. E.; Isaacs, N. W.; Reynolds, C. D.; Sakabe, K.; Sakabe, N.; Vijayan, N. M. *Philos. Trans. R. Soc., B* **1988**, *319*, 369–456.
- (5) Hermansen, K.; Fontaine, P.; Kukolja, K. K.; Peterkova, V.; Leth, G.; Gall, M.-A. *Diabetologia* **2004**, *47*, 622–629.
- (6) Kaarsholm, N. C.; Ko, H. C.; Dunn, M. F. *Biochemistry* **1989**, *28*, 4427–4435.
- (7) Smith, G. D.; Dodson, G. G. *Proteins: Struct., Funct., Genet.* **1992**, *14*, 401–408.

- (8) Derewenda, U.; Derewenda, Z.; Dodson, E. J.; Dodson, G. G.; Reynolds, C. D.; Smith, G. D.; Sparks, C.; Swenson, D. *Nature* **1989**, *338*, 594–596.
- (9) Smith, G. D.; Ciszak, E.; Magrum, L. A.; Pangborn, W. A.; Blessing, R. H. *Acta Crystallogr., Sect. D: Biol. Crystallogr.* **2000**.
- (10) Markussen, J.; Havelund, S.; Kurtzhals, P.; Andersen, A. S.; Halstrom, J.; Hasselager, E.; Larsen, U. D.; Ribel, U.; L. Schiiffer, K. V.; Jonassen, I. *Diabetologia* **1996**, *39*, 281–288.
- (11) Heise, T.; Nosek, L.; Rønn, B. B.; Endahl, L.; Heinemann, L.; Kapitza, C.; Draeger, E. *Diabetes* **2004**, *53*, 1614–1620.
- (12) (a) Jonassen, I.; Havelund, S.; Ribel, U.; Plum, A.; Loftager, M.; Hoeg-Jensen, T.; Volund, A.; Markussen, J. *Pharm. Res.* **2006**, *23*, 49–55.
(b) Jonassen, I.; Havelund, S.; Ribel, U.; Hoeg-Jensen, T.; Steensgaard, D. B.; Johansen, T.; Haahr, H.; Nishimura, E.; Kurtzhals, P. *Diabetes* **2010**, *59* (S1), A11.
- (13) Gladysz, J. A.; Curran, D. P.; Horváth, I. T. *Handbook of Fluorous Chemistry*; Wiley-VCH: Weinheim, 2004.
- (14) (a) Gottler, L. M.; de la Salud Bea, R.; Shelburne, C. E.; Ramamoorthy, A.; Marsh, E. N. G. *Biochemistry* **2008**, *47*, 9243–9250.
(b) Tang, Y.; Ghirlanda, G.; Petka, W. A.; Nakajima, T.; DeGrado, W. F.; Tirrell, D. A. *Angew. Chem. Int. Ed.*, **2001**, *40*, 1494–1496.
- (15) Glendorf, T.; Stidsen, C. E.; Norrman, M.; Nishimura, E.; Sørensen, A. R.; Kjeldsen, T. *PLoS One* **2011**, *6*, e20288.
- (16) Knaapila, M.; Svensson, C.; Barauskas, J.; Zackrisson, M.; Nielsen, S. S.; Toft, K. N.; Vestergaard, B.; Arleth, L.; Olsson, U.; Pedersen, J. S.; Cerenius, Y. J. *Synchrotron Radiat.* **2009**, *16*, 498–504.
- (17) Nielsen, S. S.; Toft, K. N.; Snakenborg, D.; Jeppesen, M. G.; Jakobsen, J. K.; Vestergaard, B.; Kutter, J. P.; Arleth, L. *J. Appl. Crystallogr.* **2009**, *42*, 959–964.
- (18) Glatter, O.; Kratky, O., Eds. *Small Angle X-ray Scattering*; Academic Press: London, 1982.
- (19) Mylonas, E.; Svergun, D. I. *J. Appl. Crystallogr.* **2007**, *40*, 245–249.
- (20) Glatter, O. *J. Appl. Crystallogr.* **1977**, *10*, 415–421.
- (21) Pedersen, S. J. Modelling of Small-Angle Scattering Data from Colloids and Polymer Systems; in *Neutrons, X-rays and Light, Scattering Methods applied to Soft Condensed Matter*, P., Lindner, Th. Zemb, Eds.; Elsevier: North-Holland, 2002.
- (22) www.pdb.org, 3I3Z.pdb 2010-05-10.
- (23) Delano, W. L. The PyMOL molecular graphics system, version 1.2r1; Schrödinger LLC, 2009.
- (24) Svergun, D., I.; Barberato, C.; Koch, M., H, J. *J. Appl. Crystallogr.* **1995**, *28*, 768–773.
- (25) Kotlarchyk, M.; Chen, S.-H. *J. Chem. Phys.* **1983**, *79*, 2461–2469.
- (26) Høiberg-Nielsen, R.; West, P.; Skov, L., K.; Arleth, L. *Biophys. J.* **2009**, *97*, 1445–1453.
- (27) Teixeira, J. J. *J. Appl. Crystallogr.* **1988**, *21*, 7781–7785.
- (28) Mittelbach, P.; Porod, G. *Acta Physica Austriaca* **1961**, *14*, 404–439.
- (29) Fournet, G. *Bull. Soc. Fr. Mineral. Crist.* **1951**, *74*, 39–113.
- (30) Arleth, L.; Bergström, M.; Pedersen, J. S. *Langmuir* **2002**, *18*, 5343–5353.
- (31) Pedersen, J. S.; Schurtenberger, P. *Macromolecules* **1996**, *29*.
- (32) Pedersen, J. S.; Laso, M.; Schurtenberger, P. *Phys. Rev. E* **1996**, *54*, R5917–R5920.
- (33) Bannwarth, W.; Knorr, R. *Tetrahedron Lett.* **1991**, *32*, 1157–1160.
- (34) Gao, J.; Mrksich, M.; Gomez, F. A.; Whitesides, G. M. *Anal. Chem.* **1995**, *67*, 3093–3100.
- (35) Tofteng, A. P.; Jensen, K. J.; Schaeffer, L.; Hoeg-Jensen, T. *ChemBioChem* **2008**, *9*, 2989–2996.
- (36) Pocker, Y.; Biswas, S. B. *Biochemistry* **1980**, *19*, 5043–5049.
- (37) Glendorf, T.; Sørensen, A. R.; Nishimura, E.; Pettersson, I.; Kjeldsen, T. *Biochemistry* **2008**, *47*, 4743–4751.
- (38) Ribel, U.; Hougaard, P.; Drejer, K. S., A. R. *Diabetes* **1990**, *39*, 1033–1039. *Diabetes* **1990**, *39*, 1033–1039.
- (39) Munch, H. K.; Heide, S. T.; Christensen, N. J.; Hoeg-Jensen, T.; Thulstrup, P. W.; Jensen, K. J. *Chem.—Eur. J.* **2011**, *17*, 7198–7204.